



Precise measurement of the energy loss spectrum of 180 GeV muons in the iron absorber of the TILECAL Module 0

TILECAL Collaboration

R. Leitner

Charles University, Prague, Czech Republic

Abstract

The energy loss spectrum of 180 GeV muons has been measured with the setup of the Module 0 and prototypes of the ATLAS hadron calorimeter in the H8 beam of the CERN SPS.

The differential probability dP/dv per radiation length of a fractional energy loss $v = \Delta E_\mu/E_\mu$ has been measured in the range $v = 0.025 \div 1.00$; it is compared with the theoretical predictions for energy losses due to bremsstrahlung and production of electron-positron pairs or of energetic knock-on electrons.

The iron elastic form factor correction $\Delta_{el}^{Fe} = 1.68 \pm 0.17_{stat} \pm 0.23_{syst} \pm 0.19_{theor}$ to muon bremsstrahlung has been measured for the first time and it is compared with different theoretical predictions.

1 Introduction

The motivation for measurements of the muon energy losses in the hadronic calorimeter of the ATLAS [1] detector as well as discussion of present experimental status ([2] [3] [4] [5] [6] [7]) has been given in Ref. [8].

In this paper, a measurement performed in 1998 with 180 GeV muons incident on a Module 0 of the ATLAS Tile Calorimeter is described and the results are compared with theoretical predictions. Large statistics of data in terms of the number of radiation lengths of iron passed by muons allowed to measure for the first time the iron nuclear elastic correction to muon bremsstrahlung process.

2 Experiment and Data Analysis

The ATLAS Tile Calorimeter is an iron-scintillator sampling calorimeter equipped with wavelength-shifting fibre readout. An important feature of this calorimeter is that the scintillator tiles are placed perpendicular to the colliding beams; a detailed description of the calorimeter concept and of the Module0 and prototypes is given elsewhere [9]. For the purpose of this measurement, the Module 0 and prototypes of the calorimeter was placed in the H8 beam of the CERN SPS, and oriented so that particles cross the tiles at perpendicular incidence (Fig. 1). In this configuration the muon beam traverses periods of an alternating towers of iron (14 mm) and scintillator (3 mm); this relatively fine granularity gives a resolution of $\sigma/E = 24\%/\sqrt{E[\text{GeV}]}$ for electromagnetic showers. The fibres collecting light from the scintillator are read out by photomultipliers and are grouped in such a way that sixteen calorimeter towers are defined. Each tower contains approximately 16 radiation lengths (X_0) of iron. In the experimental set-up, 5.6 m long Module 0 was placed on three prototypes and covered by other two prototypes from the top. The beam entered in the centre of the Module 0.

Particles of the momentum-analysed muon beam, with an energy $E_\mu = 180$ GeV, were triggered by three scintillator hodoscopes; the direction of incidence was measured by a pair of two-coordinate wire chambers. Approximately 400 000 muon triggers were used in this analysis.

A minimum-ionizing particle signal was required in scintillator hodoscopes in order to suppress trigger more than one entering particle.

Only events with the signal compatible with the beam spot of 1.5x1.5 cm in the beam chambers have been selected.

In order to eliminate very low hadron and electron contamination of the beam, the signal in calorimeter towers preceding the interaction was required to be compatible with minimum ionizing particle, i.e. only particles which have passed 6 nuclear interaction lengths and 64 radiation lengths without the interaction are selected.

Expected number of hadron induced interaction in analysed data sample is

less than 2 events. The number of muon decays in flight within the acceptance region inside the calorimeter was estimated to be 1.5 event in the accepted data sample. We have find two events (see Fig. 2) without muon escaping the shower and these events have been excluded from the analysis.

In order to ensure full containment of electromagnetic showers produced by muon radiation or knock-on electrons, only events with maximum response between the 6-th to the 13-th tower (seen by the beam) of the calorimeter were selected. In such a way all muons which started their interaction within the region of 115.3 radiation length are accepted.

The energy E_{shower} lost by muons in the calorimeter is defined in this analysis by excluding the minimum-ionization signal. It was calculated by summing the signals in three consecutive towers and subtracting the experimental value of the most probable muon signal E_{mp} in those towers (see Fig. 3).

In the previous study [8] the subtraction procedure has been simulated using GEANT 3.21. In present analysis this procedure has been checked with the data by the extrapolation of measured differential probability to zero absorber width. The energy of the shower has been evaluated as the sum of 3,4 and 5 consecutive towers respectively. The expected number of events has been found by the linear extrapolation of results to zero number of towers. Measured contribution of multiple shower events to the fractional probability dP/dv is 23%, 10%, and 2% for $v = 0.025, 0.06, \text{ and } 0.15$ respectively, as shown in Fig. 4. In the figure one may also see that subtraction of a truncated mean of the muon signal (1.7 times the most probable signal) fully eliminates multiple shower contributions. Two different methods for the definitions of ΔE_{μ} :

- $\Delta E_{\mu} = E_{\text{shower}}$ with the subtraction of the most probable signal followed by the correction of dP/dv , and

- $\Delta E_{\mu} = E_{\text{shower}}$ with the subtraction of the truncated mean signal

have been used to analyse the data. The difference of the results was included in the estimate of the systematic error.

The muon fractional energy loss was defined to be:

$$v = \Delta E_{\mu} / (E_{\mu} - \epsilon)$$

where the muon energy losses ϵ measured in towers preceding the interaction have been subtracted from the nominal beam energy.

The signal energy scale, *i.e.* the conversion factor used to obtain the energy of the signals from the digitized photomultiplier signals, was independently known for the first tower using the electron beam. The extrapolation to other towers has been done by the equalization of the most probable muon signals per one layer. The low energy muon signal has been approximated [10] by the convolution of Landau and Gaussian distribution. The precision of the most probable value is about 1% and it is highly correlated to the Cs calibration data.

The lower limit of the analysed energy loss spectrum was set to 4.5 GeV because for this value the signal from the processes studied in this paper is sufficiently well separated from the most probable muon signal.

Finally the differential probability per radiation length of a fractional energy loss in the i -th interval was calculated as

$$\frac{\Delta P}{\Delta v} = \frac{(N_i/N_{\text{tot}})}{\Delta v_i} \cdot \frac{1}{115.3X_0},$$

where N_i is the number of events in the i -th interval, N_{tot} is the total number of events passing the cuts, Δv_i is the width of the i -th interval.

The measured differential probabilities per radiation length of iron are given in Table 1 and are plotted in Fig. 5. The errors quoted are statistical only. The systematic errors of the energy loss spectrum are dominated by the uncertainty on the signal energy scale, which we take to be $\pm 1\%$, by the uncertainty on the muon energy ($\pm 1\%$), and by the uncertainty on the iron absorber thickness ($\pm 1\%$). The data have been processed with different values of the signal energy scale, of the muon energies, and of absorber thickness. The maximal positive and negative deviations of mean values were taken as systematic errors. The result is an overall systematic error on the differential probability of fractional energy loss dP/dv of $\pm 4\%$.

3 Theoretical Predictions

The theoretical predictions to be compared with these results are discussed next.

Pair production: The Kel'ner and Kotov expression [11] for the differential probability per radiation length of muon energy loss by pair production is

$$\left(\frac{dP}{dv}\right)_{\text{pair}} = C \frac{16}{\pi} Z^2 \alpha^2 \frac{1}{v} F(E_\mu, v). \quad (1)$$

The constant C is given by $C = X_0 \rho N_A r_e^2 / A = 1.185 \cdot 10^{-2}$.

Here N_A is the Avogadro constant, r_e is the classical electron radius and α is the fine structure constant; X_0 , ρ , A and Z are the radiation length, the density, the atomic weight, and the atomic number of iron. The function $F(E_\mu, v)$ is tabulated in Ref. [11] for lead and sodium at different muon energies. The interpolation of Kel'ner and Kotov's function $F(E_\mu, v)$ for the energy loss of 180 GeV muons in iron has been used.

Knock-on electrons: In order to describe the production of energetic knock-on electrons, the Bhabha formula [12] given by Rossi [13] is used (m_e is the electron mass and C as defined as above):

$$\left(\frac{dP}{dv}\right)_{\text{knock-on}} = C 2\pi Z \left(\frac{m_e}{E_\mu}\right) \frac{1 - v + \frac{v^2}{2}}{v^2} \cdot (1 + \delta_{rad}). \quad (2)$$

Here δ_{rad} is a common contribution of muon bremsstrahlung on atomic electrons and α^3 - radiative corrections to the knock-on electron production [14].

Bremsstrahlung:

The expression for the bremsstrahlung is usually written as:

$$\left(\frac{dP}{dv}\right)_{\text{bremsstrahlung}}^{\text{PS}} = C4Z^2\alpha\left(\frac{m_e}{m_\mu}\right)^2\frac{1}{v}\left(\frac{4}{3}-\frac{4}{3}v+v^2\right)\Phi(\delta(v)) \quad (3)$$

and it contains the screening function Φ .

The screening function consists of several terms:

$$\Phi = \Phi_0 - f_{coul} - \Delta_a^{el} - \Delta_n^{el} + \frac{f_a^{inel}}{Z} + \frac{f_n^{inel}}{Z} \quad (4)$$

The term Φ_0 corresponds to muon bremsstrahlung on Coulombic center in Born approximation. It has to be corrected by a subtraction of Coulomb correction f_{coul} (about 0.5% for the iron). The correction for screening of the nucleus by atomic electrons is Δ_a^{el} . The influence of nucleus formfactor is described by Δ_n^{el} . All these corrections decreases the cross section. The last two corrections accounts for the inelastic processes with atomic electrons and the nucleus. These corrections has to be taken into account in experiments, where it is impossible to separate bremsstrahlung processes without atomic and nuclear excitations. The corrections are positive, however they are suppressed by a factor $1/Z$.

Photonuclear interactions: Photonuclear interactions contribute also to the muon energy loss. The probability calculated by Bezrukov and Bugaev [15] is given by the formula from Ref. [16] (see detailed description of different terms):

$$\left(\frac{dP}{dv}\right)_{\text{photonuclear}} = C\left(\frac{A\sigma_{\gamma N}(\epsilon)}{\pi r_e^2}\right)\frac{\alpha}{2}v\Gamma(E_\mu, v), \quad (5)$$

The contribution of photonuclear interactions is about 1% for the lowest values of the fractional loss v and about 5% for the highest v value, but it is suppressed by the selection criteria. We estimated the contribution of photonuclear interactions to be about 2.5% in the region of highest energy losses.

4 Comparison of Experiment and Theory

The theoretical predictions are in very good agreement with the experimental results over the range of fractional energy loss v from 0.025 to 0.20.

The dominant process for highest muon energy losses is the bremsstrahlung. With the precise data it is therefore possible to measure the value of Δ_n^{el} . The nuclear elastic formfactor correction Δ_n^{el} is not known experimentally and there several theoretical predictions which vary from 0 to 1.5 (Ref. [14], [17], [4], [18], [19], [20] and [21]). The value of $\Delta_n^{el} = 1.5$ corresponds to approximately 20% reduction of the bremsstrahlung cross section compared to the value of $\Delta_n^{el} = 0$.

The data has been compared with theoretical prediction with the value of $\Delta_n^{el} = 0$ (see Fig. 6). The deviation from flat distribution is a signal for non zero value of Δ_n^{el} . Its value has been measured by the approximation of the data by the theoretical predictions with Δ_n^{el} being a free parameter of the approximation. The result is shown on Fig. 6.

The combined influence of systematics errors due to uncertainties in the acceptance, energy scale and multiple shower corrections is shown on Fig. 6. The other possible source of systematics errors is the limited precision of theoretical descriptions. We have assumed 3% precision in the description of pair production process. It is caused mainly by the interpolation of the function $F(E_\mu, v)$ in formula (1). The main source of uncertainties in the description of the electron knock-on process is the radiative correction δ_{rad} in formula (2). We have assumed a conservative value of 25% precision of the value of δ_{rad} . All systematic errors are summarized in the Table 2.

The value of the iron elastic nuclear formfactor correction to muon bremsstrahlung $\Delta_{el}^{Fe} = 1.68 \pm 0.17_{stat} \pm 0.23_{syst} \pm 0.19_{theor}$

has been found by the analysis of the data. This value is in agreement with the theoretical evaluation of Petrukhin and Shestakov [14, 17] and is about 5 standard deviations higher than the theoretical prediction of Ref.[19]. The comparison of the result with the theoretical predictions is given in Table 3. The value measured prefers theoretical predictions of larger value of Δ_{el}^{Fe} .

Acknowledgements

The construction of calorimeter Module 0 was only possible with substantial contributions by the technical staff of the collaborating institutions. We deeply thank them for their support.

Financial support is acknowledged from the funding agencies to the collaborating institutions.

Finally we are grateful to the staff of the SPS, and in particular to K. Elsener, for the excellent beam conditions and assistance provided during our tests.

References

- [1] ATLAS Collaboration, ATLAS Technical Proposal, report CERN/LHCC/94-43.
- [2] W. Stamm et al., *Nuovo Cim.* 51A (1979) 242.
- [3] K. Mitsui et al., *Nuovo Cim.* 73A (1983) 235.
- [4] W.K. Sakumoto et al., *Phys.Rev.* D45 (1992) 3042.
- [5] J.J. Aubert et al., *Z. Phys.* C10 (1981).
- [6] R. Kopp et al., *Z. Phys.* C28 (1985) 171.
- [7] R. Baumgart et al., *Nucl. Instrum. Methods* A258 (1987) 51.
- [8] E. Berger et al., *Z. Phys.* C73 (1997)455-463; CERN-PPE/96-115, CERN 1996.
- [9] F. Ariztizabal et al., *Nucl. Instrum. Methods* A349 (1994) 384.
E. Berger et al., report CERN/LHCC 95-44.
Atlas Collaboration, Tile Calorimeter TDR, CERN/LHCC 96-42.
- [10] T. Davidek, R. Leitner, ATLAS Internal Note ATL-TILECAL-97-114 (1997).
- [11] S.R. Kel'ner and Yu.D. Kotov, *Sov. J. Nucl. Phys.* 7 (1968) 360.
- [12] H.J. Bhabha, *Proc. Roy. Soc.* A164 (1938) 257.
- [13] B. Rossi, *High Energy Particles*, Prentice-Hall, New York, 1952.
- [14] S.R. Kelner, R.P. Kokoulin, A.A. Petrukhin, preprint 024-95, Moscow Technical University, 1995.
- [15] L.B. Bezrukov and E.V. Bugaev, *Sov. J. Nucl. Phys.* 33 (1981) 635.
- [16] W. Lohmann et al., CERN report 85-03 (1985).
- [17] A.A. Petrukhin and V.V. Shestakov, *Can. J. Phys.* 46 (1968) S377.
R.P. Kokoulin and A.A. Petrukhin, *Acta Phys. Acad. Sci. Hung.* 29 Suppl. 4 (1970) 277.
- [18] R.F. Christy, S. Kusaka, *Phys. Rev.* 59 (1941) 405.
- [19] Y. Tsai, *Rev. Mod. Phys.* 46 (1974) 815.
- [20] I.L. Rozentahl, *Usp. Fiz. Nauk*, 94 (1968) 91.
- [21] A.D. Erlykin, *Proc. 9th ICCR*, London, 2 (1966) 999.

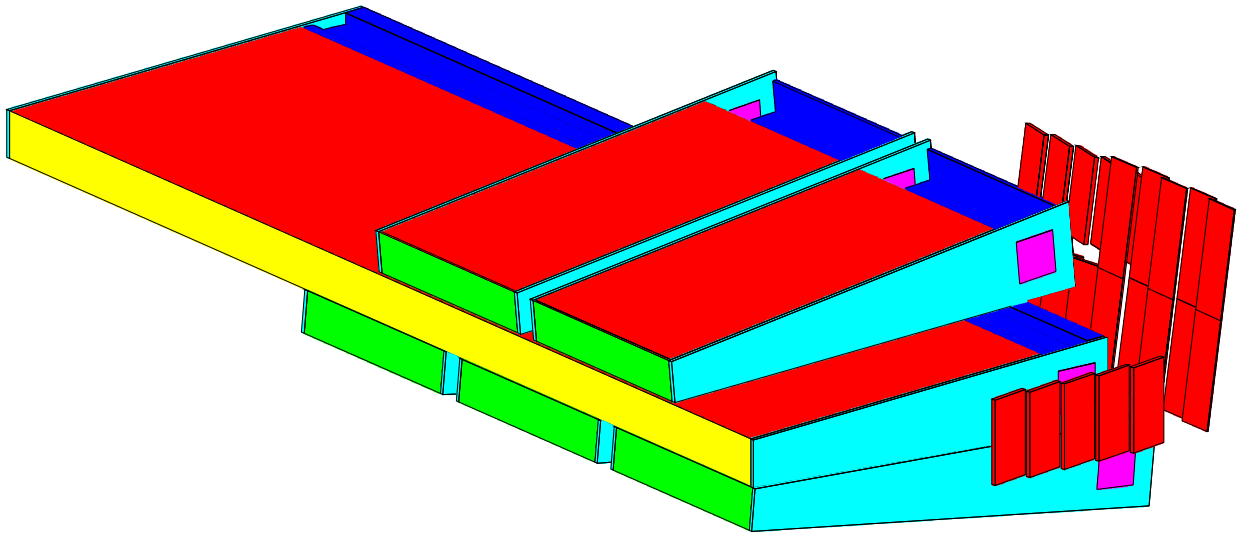


Fig. 1

The experimental setup. The beam enters the center of 5.6 m long Module 0 from the left side.

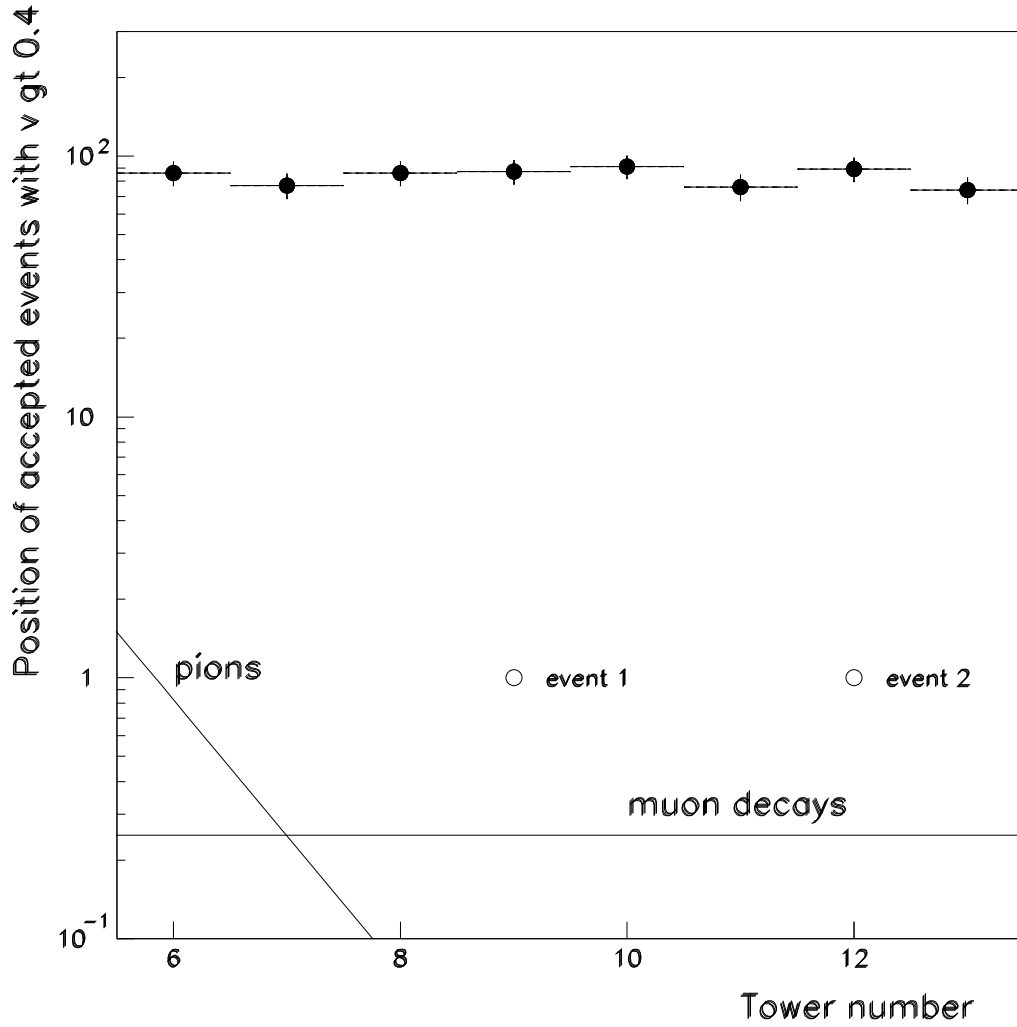


Fig. 2

Data contamination by electrons and pions. Full circles are the accepted showers with the energy larger than 70 GeV. The curves correspond to the expected contamination of the data with pion induced showers and by muon decays in flight. The empty circles indicates the two events compatible with muon decays in flight found in the data.

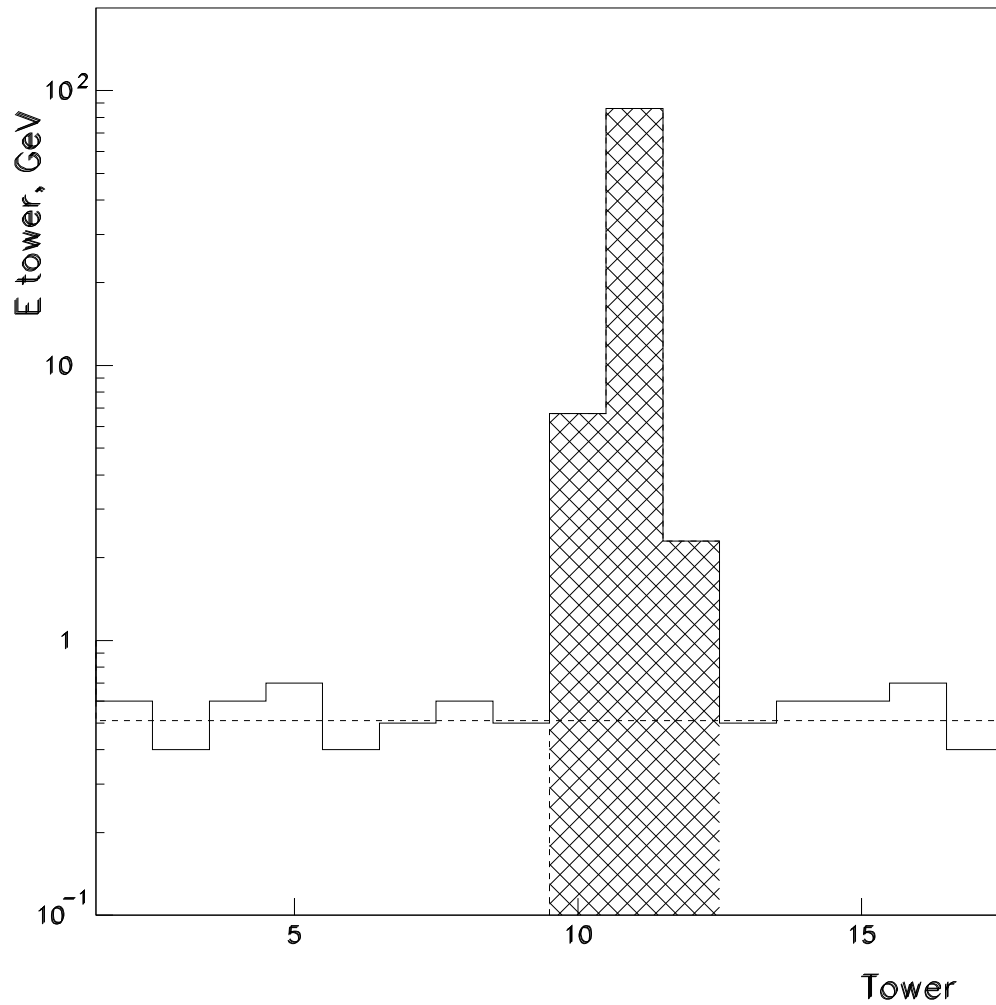


Fig. 3

An example of a 100 GeV electromagnetic shower as seen in the data. The energy E_{shower} is the sum of energies in three consecutive towers (hatched) with the most probable muon signal E_{mp} (horizontal line) subtracted.

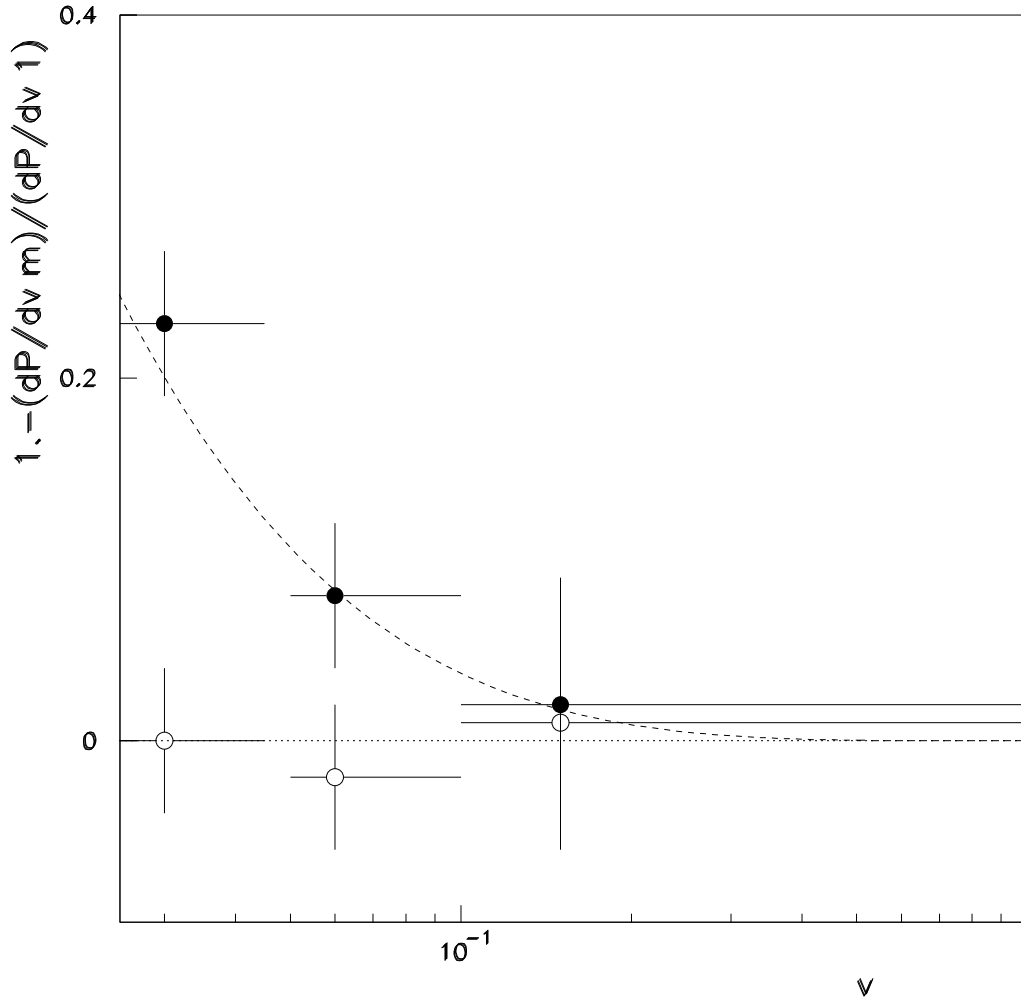


Fig. 4

A study of the multiple shower contribution to the differential probability distribution dP/dv . The full circles correspond to fractional losses defined as $v_m = (\Delta E_\mu - E_{mp})/E_\mu$, empty circles are for $v_m = (\Delta E_\mu - 1.7 \cdot E_{mp})/E_\mu$. The curve is an approximation which has been used to correct the data.

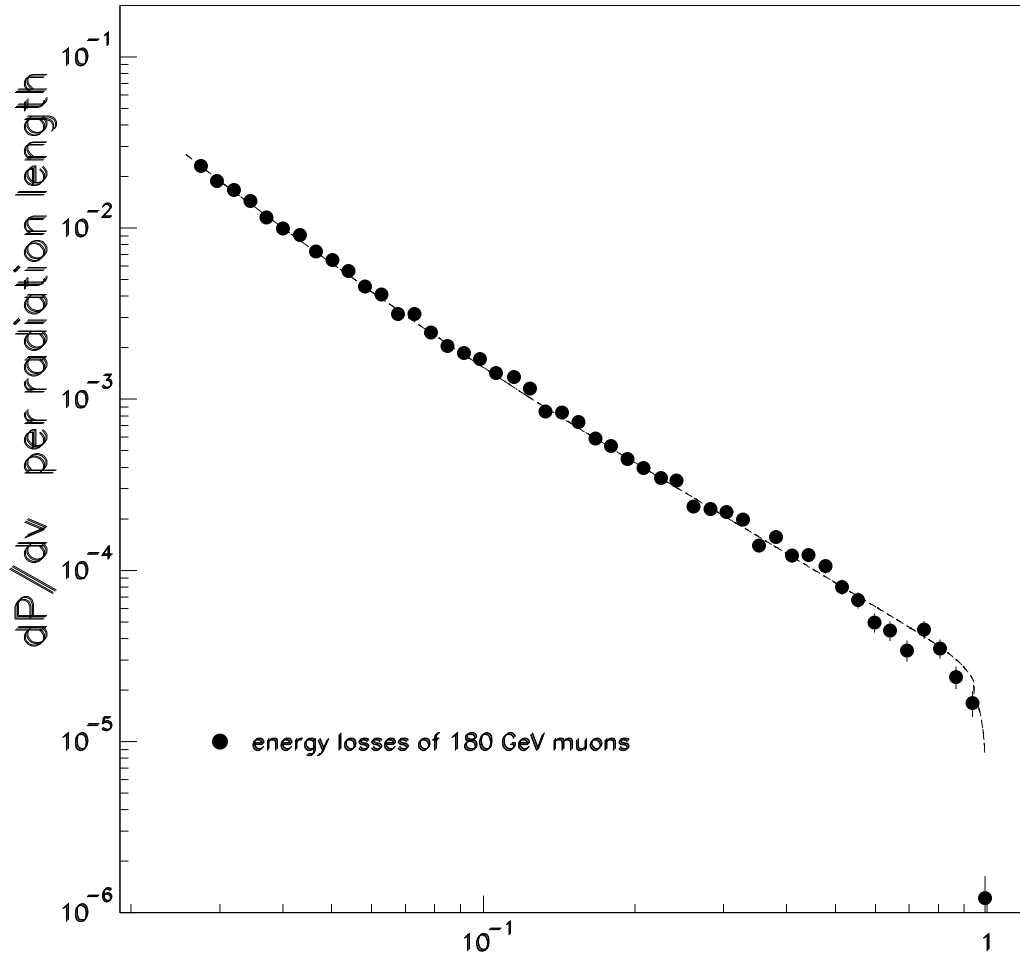


Fig. 5

The distribution of differential probabilities dP/dv for the energy loss of 180 GeV muons in iron. The full curve is the theoretical prediction described in the text.

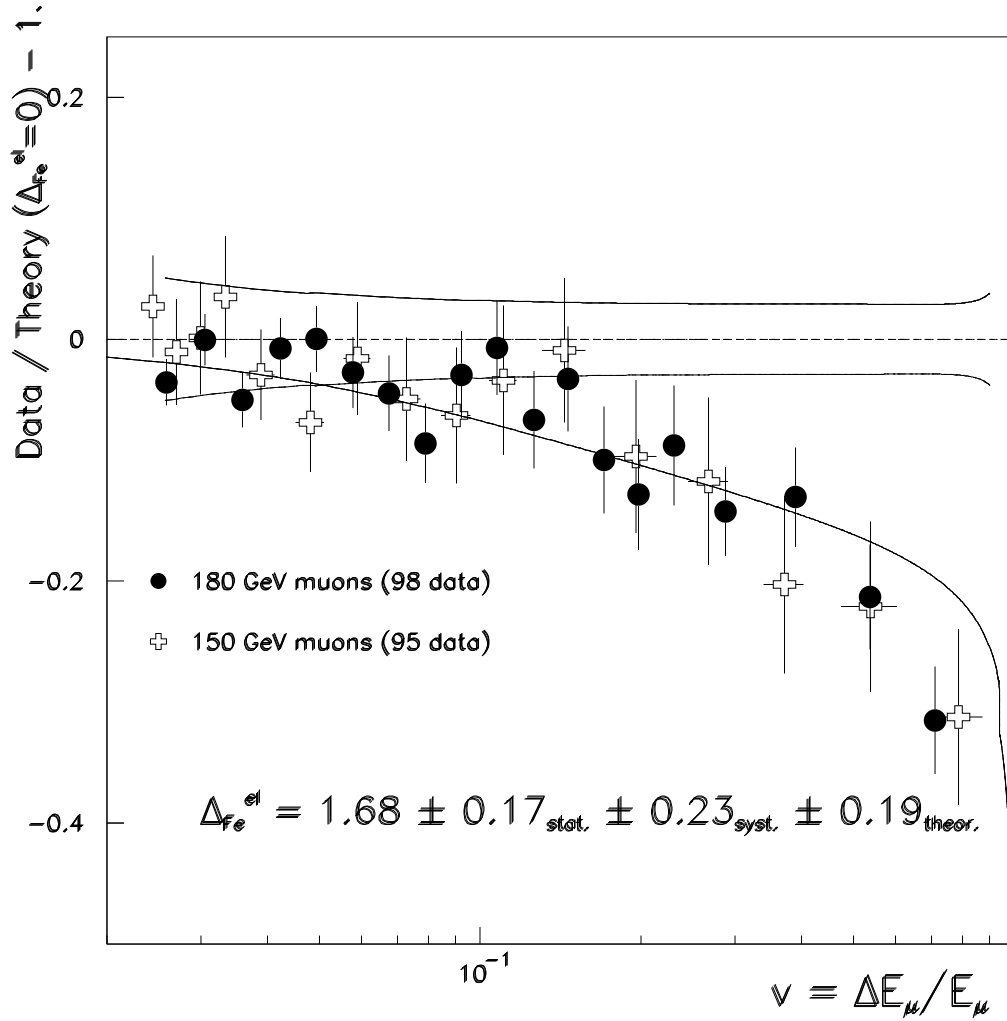


Fig. 6

The determination of Δ_{el}^{Fe} - the elastic nuclear formfactor correction to muon bremsstrahlung. The data are compared with the theoretical predictions with $\Delta_{el}^{Fe} = 0$ (horizontal line at 0) and the best approximation of the data is shown by the curve. The influence of systematic errors is shown by the two curves around the zero. For comparison, the data of Ref. [8] are plotted by crosses.

Table 1

The measured differential probability values $\Delta P/\Delta v$ for fractional muon energy losses v .

$\langle v \rangle$	$\Delta P/\Delta v$	$\langle v \rangle$	$\Delta P/\Delta v$
$(2.665 \pm 0.002) \times 10^{-2}$	$(2.31 \pm 0.06) \times 10^{-2}$	$(1.662 \pm 0.003) \times 10^{-1}$	$(5.9 \pm 0.4) \times 10^{-4}$
$(2.879 \pm 0.002) \times 10^{-2}$	$(1.89 \pm 0.05) \times 10^{-2}$	$(1.786 \pm 0.003) \times 10^{-1}$	$(5.4 \pm 0.4) \times 10^{-4}$
$(3.115 \pm 0.002) \times 10^{-2}$	$(1.67 \pm 0.05) \times 10^{-2}$	$(1.927 \pm 0.003) \times 10^{-1}$	$(4.5 \pm 0.3) \times 10^{-4}$
$(3.365 \pm 0.003) \times 10^{-2}$	$(1.45 \pm 0.04) \times 10^{-2}$	$(2.072 \pm 0.003) \times 10^{-1}$	$(4.0 \pm 0.3) \times 10^{-4}$
$(3.632 \pm 0.003) \times 10^{-2}$	$(1.16 \pm 0.04) \times 10^{-2}$	$(2.247 \pm 0.004) \times 10^{-1}$	$(3.5 \pm 0.3) \times 10^{-4}$
$(3.921 \pm 0.003) \times 10^{-2}$	$(1.00 \pm 0.03) \times 10^{-2}$	$(2.412 \pm 0.004) \times 10^{-1}$	$(3.4 \pm 0.3) \times 10^{-4}$
$(4.242 \pm 0.004) \times 10^{-2}$	$(9.2 \pm 0.3) \times 10^{-3}$	$(2.607 \pm 0.006) \times 10^{-1}$	$(2.4 \pm 0.2) \times 10^{-4}$
$(4.569 \pm 0.004) \times 10^{-2}$	$(7.3 \pm 0.3) \times 10^{-3}$	$(2.815 \pm 0.006) \times 10^{-1}$	$(2.3 \pm 0.2) \times 10^{-4}$
$(4.936 \pm 0.004) \times 10^{-2}$	$(6.5 \pm 0.3) \times 10^{-3}$	$(3.031 \pm 0.006) \times 10^{-1}$	$(2.2 \pm 0.2) \times 10^{-4}$
$(5.323 \pm 0.005) \times 10^{-2}$	$(5.6 \pm 0.2) \times 10^{-3}$	$(3.272 \pm 0.006) \times 10^{-1}$	$(2.0 \pm 0.2) \times 10^{-4}$
$(5.746 \pm 0.006) \times 10^{-2}$	$(4.6 \pm 0.2) \times 10^{-3}$	$(3.519 \pm 0.008) \times 10^{-1}$	$(1.4 \pm 0.1) \times 10^{-4}$
$(6.203 \pm 0.007) \times 10^{-2}$	$(4.1 \pm 0.2) \times 10^{-3}$	$(3.803 \pm 0.008) \times 10^{-1}$	$(1.6 \pm 0.1) \times 10^{-4}$
$(6.693 \pm 0.007) \times 10^{-2}$	$(3.2 \pm 0.2) \times 10^{-3}$	$(4.093 \pm 0.009) \times 10^{-1}$	$(1.2 \pm 0.1) \times 10^{-4}$
$(7.214 \pm 0.008) \times 10^{-2}$	$(3.2 \pm 0.1) \times 10^{-3}$	$(4.42 \pm 0.01) \times 10^{-1}$	$(1.2 \pm 0.1) \times 10^{-4}$
$(7.787 \pm 0.009) \times 10^{-2}$	$(2.5 \pm 0.1) \times 10^{-3}$	$(4.77 \pm 0.01) \times 10^{-1}$	$(1.1 \pm 0.1) \times 10^{-4}$
$(8.40 \pm 0.01) \times 10^{-2}$	$(2.1 \pm 0.1) \times 10^{-3}$	$(5.14 \pm 0.01) \times 10^{-1}$	$(8.1 \pm 0.9) \times 10^{-5}$
$(9.07 \pm 0.01) \times 10^{-2}$	$(1.9 \pm 0.1) \times 10^{-3}$	$(5.53 \pm 0.02) \times 10^{-1}$	$(6.8 \pm 0.8) \times 10^{-5}$
$(9.77 \pm 0.01) \times 10^{-2}$	$(1.73 \pm 0.09) \times 10^{-3}$	$(5.97 \pm 0.02) \times 10^{-1}$	$(5.0 \pm 0.6) \times 10^{-5}$
$(1.052 \pm 0.001) \times 10^{-1}$	$(1.43 \pm 0.08) \times 10^{-3}$	$(6.40 \pm 0.02) \times 10^{-1}$	$(4.5 \pm 0.6) \times 10^{-5}$
$(1.142 \pm 0.002) \times 10^{-1}$	$(1.35 \pm 0.07) \times 10^{-3}$	$(6.93 \pm 0.02) \times 10^{-1}$	$(3.4 \pm 0.5) \times 10^{-5}$
$(1.228 \pm 0.002) \times 10^{-1}$	$(1.16 \pm 0.07) \times 10^{-3}$	$(7.48 \pm 0.02) \times 10^{-1}$	$(4.5 \pm 0.5) \times 10^{-5}$
$(1.322 \pm 0.002) \times 10^{-1}$	$(8.5 \pm 0.6) \times 10^{-4}$	$(8.06 \pm 0.02) \times 10^{-1}$	$(3.5 \pm 0.5) \times 10^{-5}$
$(1.426 \pm 0.002) \times 10^{-1}$	$(8.4 \pm 0.5) \times 10^{-4}$	$(8.67 \pm 0.03) \times 10^{-1}$	$(2.4 \pm 0.4) \times 10^{-5}$
$(1.536 \pm 0.002) \times 10^{-1}$	$(7.4 \pm 0.5) \times 10^{-4}$	$(9.34 \pm 0.03) \times 10^{-1}$	$(1.7 \pm 0.3) \times 10^{-5}$

Table 2The sources of systematic errors of Δ_{el}^{Fe}

Source	variation of Δ_{el}^{Fe}
acceptance	0.07
energy scale	0.20
multiple showers	0.10
combined value	0.23
theoretical	0.19

Table 3

The comparison of the theoretical predictions and the measured value of the iron elastic nuclear formfactor correction Δ_{el}^{Fe} . The value of $\sigma_{\Delta_{el}^{Fe}}$ has been evaluated as the quadratic sum of statistical, systematic and theoretical errors.

Reference	Δ_{el}^{Fe}	$\frac{\Delta_{el}^{Fe}(meas) - \Delta_{el}^{Fe}(theor)}{\sigma_{\Delta_{el}^{Fe}}}$
[19] except $v \rightarrow 1.0$	0.	4.9
[4, 21]	0.52	3.4
[20]	0.65	3.0
[18]	0.90	2.3
[14, 17]	1.51, 1.49	0.5
this measurement	$1.68 \pm 0.17_{stat} \pm 0.23_{syst} \pm 0.19_{theor}$	